Renewable Power Generation Systems with Improved Active Power Filter for Performance Enhancement

Kodali Siva Krishna[1],Dr.A.Purna Chandra Rao[2]
(Prasad V. PotluriSidhartha Institute of Technology, A.P, India)[1]
(Prasad V. PotluriSidhartha Institute of Technology, A.P, India)[2]

Abstract: A simplified model predictive management methodology is presented in this paper. This methodology is based on a future reference voltage vector for a three phase four-leg voltage source inverter (VSI). Compare with the three-leg VSIs, the four-leg VSI will increase the possible switch states from 8 to 16 because of a fourth leg. Among the doable states, this could be considered within the model predictive control methodology for choosing the best state. The increased number of conducting switch states and also the corresponding voltage vectors increase the calculation burden. The proposed three-dimensional (3-D) space vector pulse width modulation (SVPWM) technique will preselect 5 among the 16 possible voltage vectors made by the three-phase four-leg voltage source inverters, based on the position of the future reference voltage vector. The discrete-time model of the future reference voltage vector is constructed to predict the future movement of the load currents, and its position is used to choose five preselected vectors at each sampling period. As a result, the proposed methodology can reduce calculation load by decreasing the voltage vectors employed in the cost function for the four-leg VSIs, while exhibiting the same performance because of the conventional methodology. The effectiveness of the projected methodology is demonstrated with simulation results.

Keywords: Three-phase four-leg optimal management, voltage supply device, 3-D SVPWM, four-leg voltage source inverter, Active power filter, predictive controller.

1 INTRODUCTION

THREE-phase four-leg voltage source inverters (VSI) will provide output voltages and current waveforms with improved quality. Compared with the three-phase three-leg VSIs, the extra fourth leg that is connected to the neutral purpose of the load will increase the switch states from 8 to 16. Traditional current management methods for the four-leg VSIs employ the proportional-integral (PI) regulator on with the pulse width modulation (PWM) stages. The carrier based mostly sinusoidal PWM method [1],[2],[3],[4],[5],[6] and 3-D space vector modulation [7],[8],[9],[10] is wide used for four-leg VSIs. With the event of high-performance microprocessors, the model predictive management technique has been recently developed as an easy and effective current management method[11],[12],[13],[14],[15],[16],[17]. This is often as a result of the method doesn't need the design of the internal current management loops, the gain regulation of the PI controllers, and therefore the use of individual PWM blocks. Additionally, the model predictive management the method will provide benefits like a quick dynamic. Because the model predictive management technique selects one optimal state when considering all the possible switching states made by a converter, the rise in the switching states of the four-leg VSIs from 8 to 16 increase the candidate switch states within the management technique, thereby increasing calculation burden.

This paper gave a simplified model predictive management method supported a future reference voltage vector for a three phase four-leg VSI. The proposed three-dimensional (3-D) spacevector pulse width modulation (SVPWM) technique will preselect 5 among the 16 possible voltage vectors made by the three phase four-leg VSI .

The management vector calculated by the digital controller within the tetrahedron defined by the boundaries of the inverter linear in operation range in abc coordinates has been conferred. A distinct approach for the three-phase four-leg VSI supported the separation of the management of the fourth leg from that of the other phases has been offered.

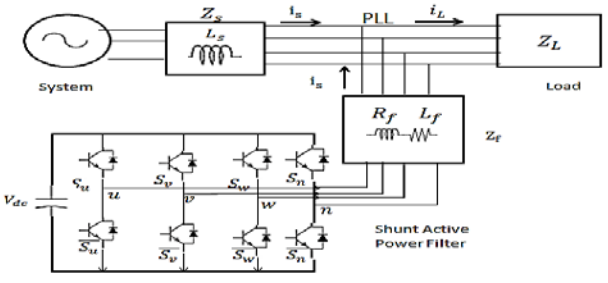

Fig.1. Three-phase equivalent circuit of the proposed shunt active power filter

A three-phase VSI has been enforced topologically by using either a three-phase three-leg inverter with split DC link capacitors or a three-phase four-leg inverter. During this study, the topology corresponding to the ability circuit utilised in the simulations and period of time applications of the three-phase four-leg VSI is the same because the one given in space vector pulse width modulation (SVPWM) is carried out by victimisation 3-D SVPWM methods in line with the

- *KODALI SIVA KRISHNA is pursuing M.tech in Power System Automation and Control in Prasad V. PotluriSidhartha Institute of Technology,Vijayawada,A.P, India.E-mail:sivakrishna.kodali5@gmail.com*
- *Dr.A.PURNA CHANDRA RAO is currently Associate professor in Prasad V. PotluriSidhartha Institute of Technology,Vijayawada,A.P, India.E-mail: rao.pvp12@gmail.com*

topology. Pulse width modulation algorithms can be utilised by creating abc coordinate transformation or directly in abc coordinates. All 3-d SVPWM available strategies using abc transformation use a 3*3 Tαβ0transformation matrix. However, phase-neutral voltages for 3-phases can't be expressed severally of every alternative in terms of modulation indices since there are four modulation indices during a 4-leg electrical converter. Consequently, electrical converter output phase-neutral voltages are calculated by subtracting the neutral leg modulation index from the modulation index of every phase. In this study,abcn to αβ0z transformation matrices used in the literature and therefore the planned 4*4 Tαβ0zOrthonormal transformation matrix has been provided during a table for 3-D SVPWM strategies.
This is often supported the position of the future reference voltage vector is established to predict the future movement of the load currents, and its position is employed to choose five preselected vectors at each sampling period. As a result, the proposed method will reduce the calculation load by decreasing the number of candidate voltage vectors utilised in the cost function for the four-leg VSIs, whereas exhibiting a similar performance as the conventional technique. The effectiveness of the proposed technique is demonstrated with simulation results.

2CONVENTIONAL MODEL PREDICTIVE CURRENT CONTROL TECHNIQUE FOR 3-PHASE 4-LEG VSI

A three-phase four-leg VSI with four legs and a general the three-phase resistive load is shown in Fig.1. Compared with a three-leg VSI , the fourth leg of the four-leg VSI connects to the neutral point of the load .The upper and lower switches in the same leg work with a complementary operation. Thus, the output phase voltage of the 4-leg VSI is determined depending on the switching states of the upper switches(s=d), d_u , d_v , $d_w$and d_n. Each upper switch assumes a binary value of "1" and "0" in the closed and open states, respectively , and 16 switching states are generated by the 4-leg VSI.

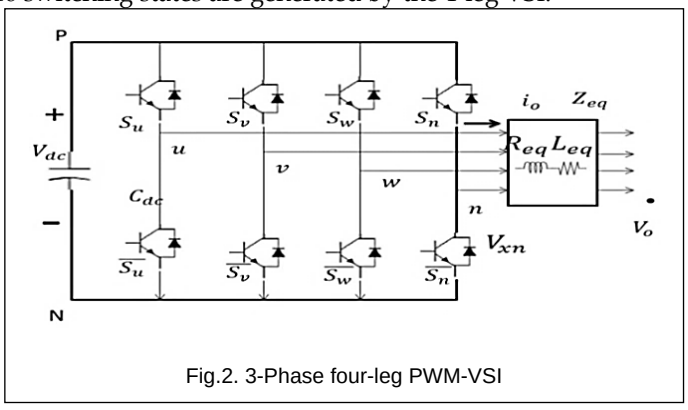

Fig.2. 3-Phase four-leg PWM-VSI

In the conventional model predictive management technique of the 4-leg VSI, the future current movements at the (k+1)thstep according to the 16 possible switch states are predicted using the current prediction, one optimum switching state is selected through a cost function that minimises the load current error between the future reference and predicted currents. For simplicity, the three-phase output voltages and currents are represented as vectors:

(1) $V=[\,Van\;\; VbnVcn]^T$

(2) $I=[IaIbIc]^T$

The load current dynamics of the 4-leg VSI in Fig.2 is described as

(3) $$v_{xn} = d_x - d_n v_{dc}, \qquad x = u, v, w, n$$

(4) $$v_{xn}=\begin{bmatrix} v_{an} \\ v_{bn} \\ v_{cn} \\ v_{nn} \end{bmatrix}=\begin{bmatrix} 1 & 0 & 0 & -1 \\ 0 & 1 & 0 & -1 \\ 0 & 0 & 1 & -1 \\ 0 & 0 & 0 & 0 \end{bmatrix}\begin{bmatrix} d_u \\ d_v \\ d_w \\ d_n \end{bmatrix} * V_{dc}$$

The mathematical model of the filter derived from the equivalent circuit shown in Fig. 2 is

(5) $$v_o = v_{xn} - R_{eq} i_o - L_{eq} \frac{di_o}{dt}$$

Where Req and Leq are the equivalent resistance and inductance, respectively. Therefore, thevenin equivalent impedance is decided by a series connection of the ripple filter impedance Z_f and a parallel arrangement between the system equivalent impedance Z_s and therefore the load impedanceZ_L.

(6) $$Z_{eq} = \frac{Z_s Z_L}{Z_s + Z_L} + Z_f \approx Z_s + Z_f$$

For this model, it is assumed that $Z_L \gg Z_s$, that the resistive part of the system's equivalent impedance is neglected, which the series reactance is vary within the 3–7% p.u. that is an appropriate approximation of the real system. Finally, in (5), $R_{eq} = R_f$ and $L_{eq} = L_s + L_f$.

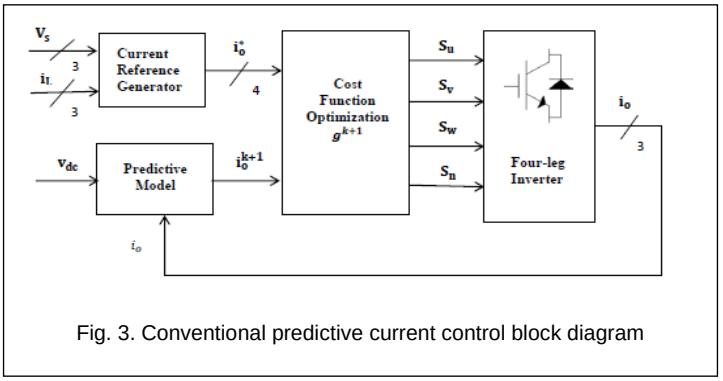

Fig. 3. Conventional predictive current control block diagram

The derivative of the load current with respect to time in (5) will be approximated within the discrete-time domain as

(7) $$\frac{dx}{dt} \approx \frac{i(k+1) - i(k)}{T_s}$$

As a result, the one-step future load current is expressed in the discrete-time type as, from Eq.(5) and (7)

$$I_o[k+1] = \frac{T_s}{L_{eq}}(v_{xn}[k] - V_o[k]) \qquad (8)$$

The future reference current at the (k+1)th step, for a requirement of the load current management methodology is

obtained using the current reference generator. Assume reference current value is (k)th step and (k+1)th step is same valuei*(k+1)=i*(k).The Possible switching states and the corresponding output phase voltages of the 4-leg inverter

TABLE I

Switching states	V_{an}	V_{bn}	V_{cn}
pppp	0	0	0
nnnp	-Vdc	-Vdc	-Vdc
pnnp	0	-Vdc	-Vdc
ppnp	0	0	-Vdc
npnp	-Vdc	0	-Vdc
nppp	-Vdc	0	0
nnpp	-Vdc	-Vdc	0
pnpp	0	-Vdc	0
pppn	Vdc	Vdc	Vdc
nnnn	0	0	0
pnnn	Vdc	0	0
ppnn	Vdc	Vdc	0
npnn	0	Vdc	0
nppn	0	Vdc	Vdc
nnpn	0	0	Vdc
pnpn	Vdc	0	Vdc

Table I shows the 16 possible output voltage vectors generated by the four-leg VSI, depending on the switching states, wherever the 'P' and 'n' states of every leg implies that the upper and also the lower switch of the corresponding leg is in the On state. Table Iadditionally indicates that the load current at the (k+1)th step in (8) is predicted according to the voltage vector determined by the 16 switching states. Among the 16 possibilities for the future load current at the (k+1)th step, an optimalpredicted current which will minimise the error between the reference and predicted load currents is decided by the cost function is given by

$$g[k+1]= (i^*_{ou}[k+1] - i_{ou}[k+1])^2 + (i^*_{ov}[k+1] - i_{ov}[k+1])^2$$

$$+(i^*_{ow}[k+1] - i_{ow}[k+1])^2 + (i^*_{on}[k+1] - i_{on}[k+1])^2 \quad (9)$$

Note that the three-phase four leg VSI needs 16 repeated calculations to find the optimal switching state resulting in the optimal predicted current. Fig.3. diagram of the conventional model predictive control methodology for the three-phase four-leg VSI. If the[pppp] state or the [nnnn] state is chosen because of the cost function, the switching state ought to be determined by considering the switching loss. For example, in case the present switching state is [ppnp], and the [pppp] state or the [nnnn] state is chosen as a result of the cost function, [pppp] should be used at the (k+1)th step to cut back the number of phases involved with the commutation in (9). The conventional model predictive current management methodology algorithm for the three-phase four-leg VSI isin (4).

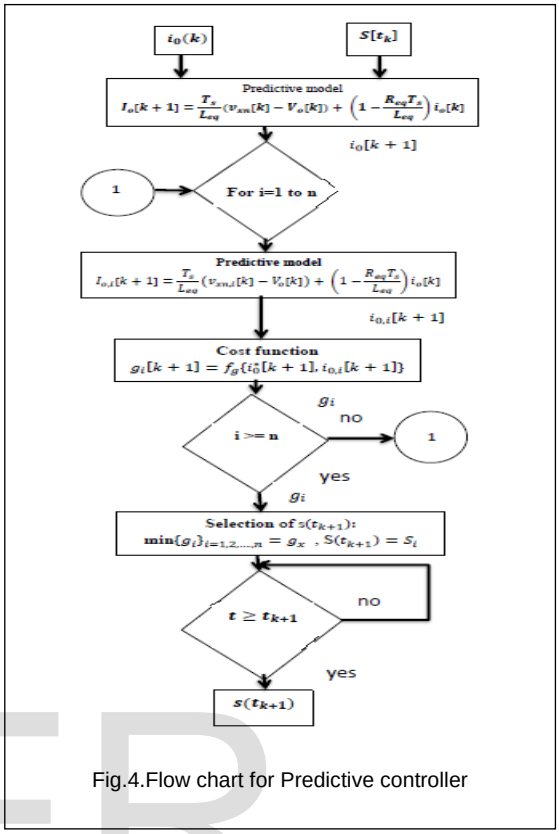

Fig.4.Flow chart for Predictive controller

The input values taken as i_0 , d[t_k] predefined values of the compensating current and switching state. Based on these values the predictive control block calculates the i_0[k+1] value, repeat the processuntil 16 predictive values. Reference current values calculate from dq-base reference current method and compare those values predictive values using.

2.1 dq-Base Current Reference Generator

A dq-based current reference generator scheme is used to obtain the active power filter current reference signals. The dq-base scheme has fast accurate, response and signal tracking capability.dq- based current reference generator scheme characteristic avoids voltage fluctuations that deteriorate the current reference signal performance of compensation. The reference current signals are obtained from the corresponding load currents as shown in Fig .5.

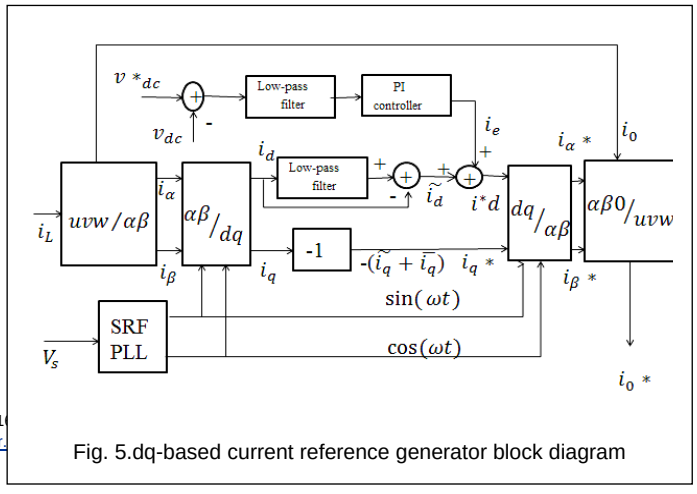

Fig. 5.dq-based current reference generator block diagram

The dq-based scheme operates in rotating reference theory. The currents measured must be multiplied by the sin(ωt) andcos(ωt) signals. By using dq-transformation, the d-axis current component is synchronized with the corresponding phase-to-neutral system voltage, and the q-axis current component is phase-shifted by 900. The sin(ωt) and cos(ωt) synchronized reference signals are obtained from a synchronous reference frame (SRF). The SRF-PLL generates a pure sinusoidal waveform even when the system voltage is severely distorted. Tracking errors are eliminated.

The dq-transformation, transforms the three-phase stationary coordinate system to the dq rotating coordinate system.

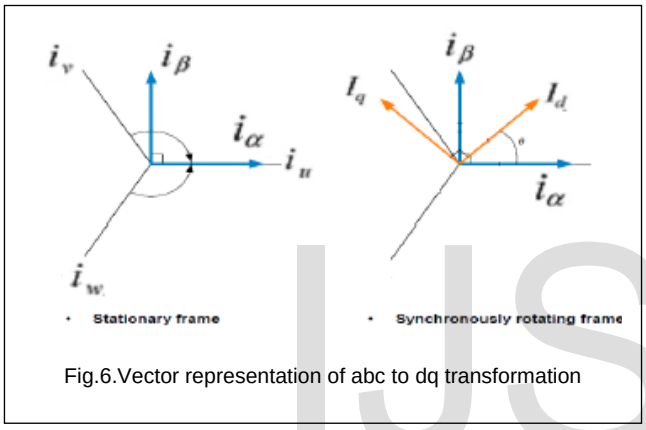

Fig.6.Vector representation of abc to dq transformation

This transformation is done two steps:

The three-phase stationary transformation of coordinate system to the two-phase so-called αβ stationary coordinate system and

A transformation from the αβ stationary coordinate system to the αβ rotating coordinate system.

From Fig.6. Vector representation of abc to dq transformation to transform the abc to αβ using Clark transformation shown in Eq. (11)

$$\begin{bmatrix} i_d \\ i_q \end{bmatrix} = \sqrt{\frac{2}{3}} \begin{bmatrix} \sin\theta & \cos\theta \\ -\cos\theta & \sin\theta \end{bmatrix} \begin{bmatrix} i_\alpha \\ i_\beta \end{bmatrix} \quad (10)$$

αβ to dq using park transformation in Eq.(10)

$$\begin{bmatrix} i_d \\ i_q \end{bmatrix} = \sqrt{\frac{2}{3}} \begin{bmatrix} \sin\theta & \cos\theta \\ -\cos\theta & \sin\theta \end{bmatrix} \begin{bmatrix} 1 & -\frac{1}{2} & -\frac{1}{2} \\ 0 & \frac{\sqrt{3}}{2} & -\frac{\sqrt{3}}{2} \end{bmatrix} \quad (11)$$

The transformation from abc to dq in Eq.(12)

$$\begin{bmatrix} i_\propto \\ \cdot \end{bmatrix} = \sqrt{\frac{2}{}} \begin{bmatrix} 1 & -\frac{1}{2} & -\frac{1}{2} \end{bmatrix} \begin{bmatrix} i_u \\ i_{\cdot\cdot} \end{bmatrix} \quad (12)$$

A low-pass filters (LFP) using in Fig.5 to extracts the dc component of the phase currents id to generate the harmonic reference components –iq. The reactive reference components of the phase-currents are obtained by phase-shifting the corresponding ac and dc components of $-i_q$ by 1800. In order to keep the dc-voltage constant the amplitude of the converter reference current must be modified by adding an active power reference signal i_e with the d-component. The resulting signals id* and i_q* are transformed back to a three-phase system by applying the inverse Park and Clark transformation as shown in Eq.(13)

(13)

The current that flows through the neutral of the load is compensated by injecting an analogous instant value obtained from the Phase-currents, phase-shifted by180^o, as shown next.

$$i^*_{on} = -(i_{Lu} + i_{Lv} + i_{Lw}) \quad (14)$$

One of the key advantages of the dq-based current reference generator theme is that it permits the implementation of a linear controller among the dc-voltage control loop. However, one necessary disadvantage of the dq-based current arrangement formula used to generate the present reference is that a second order harmonic part is generated in i_d and i_q underneath unbalanced in operation conditions.

3 Proposed Model Predictive Control Method Using 3-D SVPWM

In this section, the proposed 4*4 Tαβ0z orthonormal transformation matrix in the three-phase four-leg electrical convertor for 3-D SVPWM strategies are given and the nonzero switch space vectors from which projection matrices are determined are derived for the new matrix by using the topology in Fig.2. Depending on the 16 switching cases. Within the topology in Fig.2, Vin are electrical converter output phase-neutral voltage and di ,(i=u;v;w;n) are modulation indices taking values in[0,1]. Then unaltered section voltages are found as

Vun=Vug-Vng
Vvn=Vvg-Vng
Vwn=Vwg-Vng

$$V_{ig} = \begin{bmatrix} V_{ug} \\ V_{vg} \\ V_{wg} \\ V_{ng} \end{bmatrix} = \begin{bmatrix} 1 & 0 & 0 & 0 \\ 0 & 1 & 0 & 0 \\ 0 & 0 & 1 & 0 \\ 0 & 0 & 0 & 1 \end{bmatrix} \begin{bmatrix} d_u \\ d_v \\ d_w \\ d_n \end{bmatrix} V_{dc} \quad (15)$$

$$V_{in} = \begin{bmatrix} V_{un} \\ V_{vn} \\ V_{wn} \\ V_{nn} \end{bmatrix} = \begin{bmatrix} 1 & 0 & 0 & -1 \\ 0 & 1 & 0 & -1 \\ 0 & 0 & 1 & -1 \\ 0 & 0 & 0 & 0 \end{bmatrix} \begin{bmatrix} d_u \\ d_v \\ d_w \\ d_n \end{bmatrix} V_{dc}$$

The place holder Vnn is defined to form a 4*4 transform. As will be seen from the higher than Vig matrix in Eq.(15), the

modulation indices of electrical converter legs are independent of every other. Since the matrix between V_{in} and d_i is 3*4 , the classical 3*3 $T_{\alpha\beta 0}$ transformation matrix for abc to αβ0 transformation cannot be used. For this reason, the unaltered phase voltages are obtained by using the following expression in studies within the literature.

$$\begin{bmatrix} V_{un} \\ V_{vn} \\ V_{wn} \end{bmatrix} = \begin{bmatrix} d_u - d_n \\ d_v - d_n \\ d_w - d_n \end{bmatrix} V_{dc} \qquad (17)$$

Hence, modulation indices d_u,d_v,d_w are defined in terms of d_n and the 3*3 $T_{\alpha\beta 0}$ transformation matrix will be used. As a brand new approach, abcn to αβ0z transformation and 4*4 $T_{\alpha\beta 0z}$ orthonormal transformation matrix are defined and used, giving rise to independence of modulation indices from d_n. Details of the 4*4 orthogonal transformation matrix will be found in (8,16). The orthonormal transformation matrix $T_{\alpha\beta 0z}$ is given as

$$T_{\alpha\beta 0z} = \sqrt{\frac{2}{3}} \begin{bmatrix} 1 & -(1/2) & -(1/2) & 0 \\ 0 & \sqrt{3}/2 & -(\sqrt{3}/2) & 0 \\ (1/(2*\sqrt{2})) & (1/(2*\sqrt{2})) & (1/(2*\sqrt{2})) & -(3/(2*\sqrt{3})) \\ (\sqrt{3}/(2*\sqrt{2})) & (\sqrt{3}/(2*\sqrt{2})) & (\sqrt{3}/(2*\sqrt{2})) & (\sqrt{3}/(2*\sqrt{2})) \end{bmatrix} \qquad (18)$$

The $T_{\alpha\beta 0z}$ matrix transforms phase-voltages space into an equivalent 3-degree of freedom (DOF) orthonormal output voltage space and V_z is defined as a placeholder for the loss of 1-DOF. The $T_{\alpha\beta 0z}$ matrix is orthonormal and invertible, i.e. $T_{\alpha\beta 0z} = T^{T}_{\alpha\beta 0z}$=I. Therefore, the row and column vectors from a basis for the 4-DOF leg- voltage space. Let $V_{\alpha\beta 0z}$ and V_{abcn} be defined as

$$V_{\alpha\beta 0z} = [V_\alpha \; V_\beta V_0 V_z]^T$$
$$V_{abcn} = [V_a \; V_b V_c V_n]^T$$

Then abcn to αβ0z transformation is given bellow

$$V_{\alpha\beta 0z} = T_{\alpha\beta 0z} * V_{abcn}$$

$$V_{\alpha\beta 0z} = T_{\alpha\beta 0z} * \begin{bmatrix} 1 & 0 & 0 & -1 \\ 0 & 1 & 0 & -1 \\ 0 & 0 & 1 & -1 \\ 0 & 0 & 0 & 0 \end{bmatrix} \begin{bmatrix} d_u \\ d_v \\ d_w \\ d_n \end{bmatrix} V_{dc}$$

Rearranging the above expression gives

$$V_{\alpha\beta 0z} = \begin{bmatrix} \frac{1}{\sqrt{6}}(2d_u - d_v - d_w) \\ \frac{1}{\sqrt{2}}(d_v - d_w) \\ \frac{1}{2\sqrt{3}}(d_u + d_v + d_w - 3d_n) \\ \frac{1}{2}(d_u + d_v + d_w - d_n) \end{bmatrix} V_{dc}$$

$d_{\alpha\beta 0z}$ is defined as follows;

$$\begin{bmatrix} d_\alpha \\ d_\beta \\ d_0 \\ d_z \end{bmatrix} = \begin{bmatrix} 2 & -1 & -1 & 0 \\ 0 & 1 & -1 & 0 \\ 1 & 1 & 1 & -3 \\ 1 & 1 & 1 & -1 \end{bmatrix} \begin{bmatrix} d_u \\ d_v \\ d_w \\ d_n \end{bmatrix}$$

$V_{\alpha\beta 0z}$, transform expression can be written in terms of modulation indices as

$$\begin{bmatrix} V_\alpha \\ V_\beta \\ V_0 \end{bmatrix} = \begin{bmatrix} \frac{1}{\sqrt{6}} d_\alpha \\ \frac{1}{\sqrt{2}} d_\beta \\ 2 \end{bmatrix} V_{dc}$$

(24)

The switching combinations of d_{uvwn} , their transformations, and sixteen switching states vectors. Space vector corresponding to 16 switch cases given in Table 2 are represented in Fig.7 & 8 as 3-D vectors .

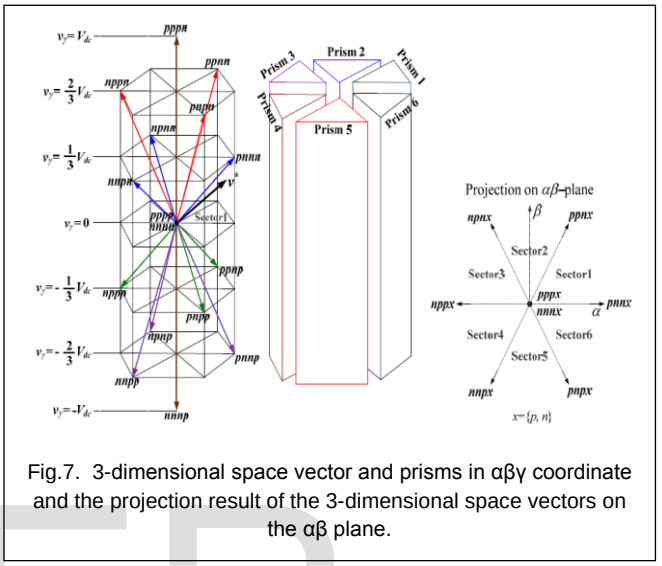

Fig.7. 3-dimensional space vector and prisms in αβγ coordinate and the projection result of the 3-dimensional space vectors on the αβ plane.

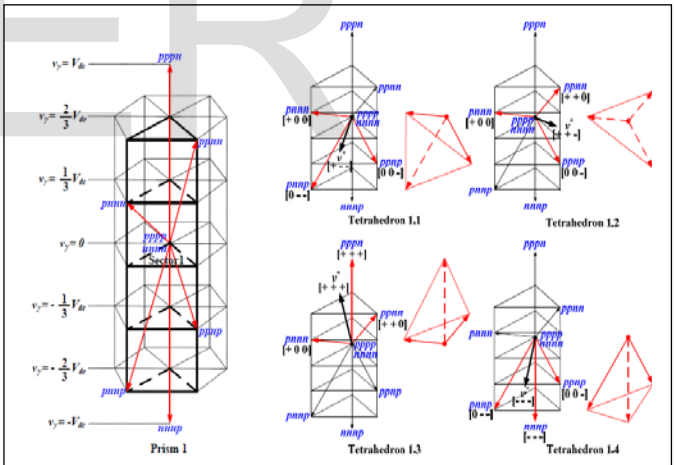

Fig.8. Example of the vector preselection technique with the reference voltage vector in Prism 1.

3.1 Three-D SVPWM for four-leg VSI

At any given instant, the section voltages at the output of the four-leg VSI could be made by an equivalent switching state vectors and calculation of duty cycles identification of adjacent vectors could be a two-step process.

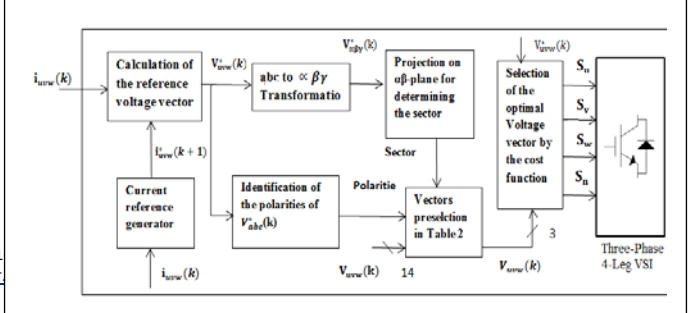

Fig.9. Block diagram of the proposed 3-D SVPWM method.

This method determines the position of the reference voltage at every sampling instant. Based on the position of the reference voltage, three active voltage vectors surrounding the reference voltage vector can be preselected among the entire This paper proposes a model predictive control method based on a vector pre-selection technique for the three-phase four-leg VSI to find the voltage vector closest to the reference voltage vector. 14 active voltage vectors generated by the three-phase four-leg VSI, as shown in Fig.9.

In addition tothe three preselected active voltage vectors, two zero vectors corresponding to the switching states, [pppp] and [nnnn], are included as optimal voltage vector candidates. As a result, only five vectors surrounding the reference voltage vector canbe judged as candidates for the optimal voltage vector based on the position of the reference voltage vector at every sampling period, without considering all the 16 voltage vectors generated by the three-phase four-leg VSI. Thus, the calculation burden for determining the optimal voltage vectorclosest to the reference voltage vector can be reduced from 16 to 5 calculations. As a result, the proposed method can demonstratethe same performance as the conventional model predictive control method with reduced calculation burden.

3.1.1 Identification of the prism number:

The vectors space givenFig.8. is split into six triangular prisms(p1-p6) shown in Fig.7.Let the reference vector voltage that produces the required phase voltage at the inverter output be in any prism as shown in Fig.10. Then the algorithm used to determine the prism range is shown in Fig.10

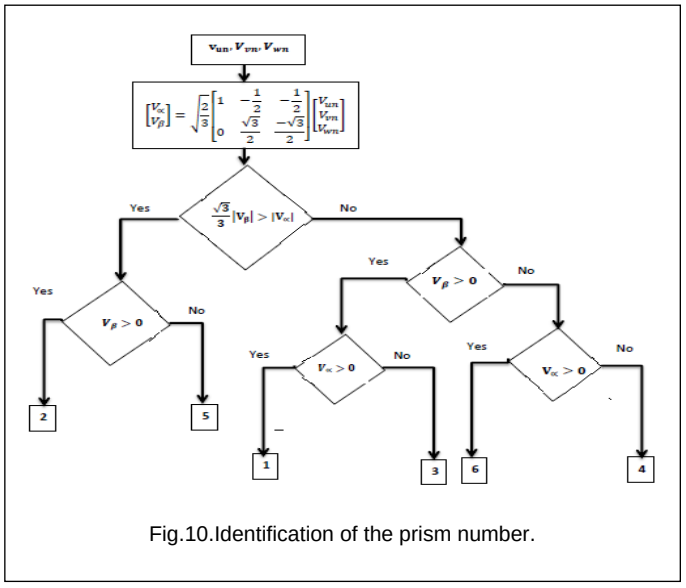

Fig.10.Identification of the prism number.

3.1.2 Identification of polyhedron:

The second step is to work out the tetrahedron during which the reference vector is present. Every prism is split into four tetrahedrons, resulting in a total of 24 tetrahedrons. Every tetrahedron has 3 non-zero switching state vectors (NZSVs) and two zero switching state vectors (ZSVs). There is no mathematical expression for determining the tetrahedron containing the reference space vector within the space. Fortunately, supported the voltage polarities of the reference vectors in abccoordinate$[V_{uref} \quad V_{vref} \quad V_{wref}]^T$, the tetrahedrons will be simply determined. Table 2 lists all possible polarities of the reference voltages to work out the tetrahedrons and the connected 3 adjacent NZSVs.

TABLE 2

Prism	Tetrahedrons	Active Vectors	Condition
P1	T1	ppnp,pnnp,pnnn	Vu>0,Vv<0,Vw<0
	T2	pnnn,ppnn,ppnp	Vu>0,Vv>0,Vw<0
	T13	nnnp,pnnp,ppnp	Vu<0,Vv<0,Vw<0
	T14	pppn,ppnn,pnnn	Vu>0,Vv>0,Vw>0
P2	T3	npnn,ppnn,ppnp	Vu>0,Vv<0,Vw<0
	T4	ppnp,npnp,npnn	Vu>0,Vv>0,Vw<0
	T15	nnnp,npnp,ppnp	Vu<0,Vv<0,Vw<0
	T16	pppn,ppnn,npnn	Vu>0,Vv<0,Vw<0
P3	T5	nppp,npnp,npnn	Vu>0,Vv>0,Vw>0
	T6	npnn,nppn,nppp	Vu<0,Vv>0,Vw>0
	T17	nnnp,npnp,nppp	Vu<0,Vv<0,Vw<0
	T18	pppn,npnn,nppn	Vu>0,Vv>0,Vw>0
P4	T7	nnpn,nppn,nppp	Vu<0,Vv>0,Vw>0
	T8	nppp,nnpp,nnpn	Vu<0,Vv<0,Vw>0
	T19	nnnp,nnpp,nppp	Vu<0,Vv<0,Vw<0
	T20	pppn,nppn,nnpn	Vu>0,Vv>0,Vw>0
P5	T9	pnpp,nnpp,nnpn	Vu<0,Vv<0,Vw>0
	T10	nnpn,pnpn,pnpp	Vu>0,Vv<0,Vw>0
	T21	nnnp,pnpp,nnpp	Vu<0,Vv<0,Vw<0
	T22	pppn,nnpn,pnpn	Vu>0,Vv>0,Vw>0
P6	T11	pnnn,pnpn,pnpp	Vu>0,Vv<0,Vw>0
	T12	pnpn,pnpn,pnnn	Vu>0,Vv<0,Vw<0
	T23	nnnp,pnnp,pnpp	Vu<0,Vv<0,Vw<0
	T24	ppnp,pnnn,pnpn	Vu>0,Vv>0,Vw>0

3.1.3Calculation of duty cycles:

The reference vector Vref corresponding to the active vectors connected to the tetrahedron obtained in Table 2 is set from Table 1 as

$$V_{ref} = [V_{uref} \quad V_{vref} \quad V_{wref}]^T$$

Duty ratios of the switch vectors for this reference vector are given by

$$\begin{bmatrix} d_u \\ d_v \\ d_w \end{bmatrix} = \frac{1}{V_{dc}} [V_1 \quad V_2 \quad V_3]^{-1} \begin{bmatrix} V_{uref} \\ V_{vref} \\ V_{wref} \end{bmatrix}$$

$$d_n = 1 - (d_u + d_v + d_w)$$

As an example, let the reference vector $[V_{uref} \quad V_{vref} \quad V_{wref}]^T$ be in prism 2 and also the corresponding tetrahedron be 4(T3).

From Table 2, the connected switch vectors are V_1 = npnn, V_2 = ppnn , V_3 = ppnp , V_0 = [pppp, nnnn]. The modulation indices are calculated by using Table 3 following expression:

$$\begin{bmatrix} d_u \\ d_v \\ d_w \end{bmatrix} = \frac{1}{V_{dc}} \begin{bmatrix} -1/\sqrt{6} & 1/\sqrt{6} & 1/\sqrt{6} \\ -1/\sqrt{2} & 1/\sqrt{2} & 1/\sqrt{2} \\ 1/\sqrt{3} & 2/\sqrt{3} & -1/\sqrt{3} \end{bmatrix}^{-1} \begin{bmatrix} V_{uref} \\ V_{vref} \\ V_{wref} \end{bmatrix} \quad (27)$$

Table-3

n	d_{abcn}	$d_{\alpha\beta 0}$	Vn= $\begin{bmatrix} d_\alpha/\sqrt{6} & d_\beta/\sqrt{2} & d_0/(2*\sqrt{3}) \end{bmatrix}^T$ Vdc
0	nnnn	0 0 0	$V_0 = [0\ 0\ 0]^T * Vdc$
1	nnnp	0 0 -3	$V_1 = [0\ 0\ -\sqrt{3}/2]^T * Vdc$
2	nnpn	-1-1 -1	$V_2 = \left[-\frac{1}{\sqrt{3}} - 1/\sqrt{2}\ 1/(2*\sqrt{3})\right]^T$ Vdc
3	nnpp	-1-1 -2	V3= $\left[-1/\sqrt{6} \quad -1/\sqrt{2} \quad -2/(2*\sqrt{3})\right]^T$ Vdc
4	npnn	-1 1 1	V4= $\left[-1/\sqrt{6} \quad 1/\sqrt{2} \quad 1/(2*\sqrt{3})\right]^T$ Vdc
5	npnp	-1 1 -2	V5= $\left[-1/\sqrt{6} \quad 1/\sqrt{2} \quad -2/(2*\sqrt{3})\right]^T$ Vdc
6	nppn	-2 0 2	V6=$\left[-2/\sqrt{6} \quad 0 \quad 2/(2*\sqrt{3})\right]^T$ Vdc
7	nppp	-2 0 -1	V7=$\left[-2/\sqrt{6} \quad 0 \quad -1/(2*\sqrt{3})\right]^T$ Vdc
8	pnnn	2 0 1	V8=$\left[2/\sqrt{6} \quad 0 \quad 1/(2*\sqrt{3})\right]^T$ Vdc
9	pnnp	2 0 -2	V9= $\left[2/\sqrt{6} \quad 0/\sqrt{2} \quad -2/(2*\sqrt{3})\right]^T$ Vdc
10	pnpn	1 -1 2	V10= $\left[1/\sqrt{6} \quad -1/\sqrt{2} \quad 2/(2*\sqrt{3})\right]^T$ Vdc
11	pnpp	1 -1 -1	V11= $\left[1/\sqrt{6} \quad -1/\sqrt{2} \quad -1/(2*\sqrt{3})\right]^T$ Vdc
12	ppnn	1 1 2	V12= $\left[1/\sqrt{6} \quad 1/\sqrt{2} \quad 2/(2*\sqrt{3})\right]^T$ Vdc
13	ppnp	1 1 -1	V13= $\left[1/\sqrt{6} \quad 1/\sqrt{2} \quad -1/(2*\sqrt{3})\right]^T$ Vdc
14	pppn	0 0 3	V14=$\left[0 \quad 0 \quad 3/(2*\sqrt{3})\right]^T$ Vdc
15	pppp	0 0 0	V15=$[0\ 0\ 0]^T$Vdc

In summary, time duration of the selected switching vectors are calculated by using 4*4 $T_{\alpha\beta 0z}$ orthonormal transformation matrices as a new approach for 3-D SVPWM strategies.

The discrete-time modelling of the load current dynamics in (8); this is often accomplished by assuming that the one-step future load currents become adequate to the one-step future current references by applying the voltage reference. A more sophisticated discrete-time modelling for reference voltage production may be obtained by discretization supported a lot of subtle methods, rather than the approximation according to a backwards finite-difference technique. The discrete time state-space equation can be represented as

$$\dot{x(t)} = A\,x(t) + B\,u(t) \quad (28)$$

$$\dot{x}(t) = \lim_{T\to 0} \frac{x(t+T_s) - x(t)}{T_s}$$

$$x((k+1)T_s) = (I + T_s A)\,x(kT_s) + T_s B u(kT_s) \quad (29)$$

In a discrete-time domain where the input variables change value only at discrete time instants kTs , the state equation based on exact discrete-time model may be written by

$$X(k+1) = A_d x(k) + B_d u(k)$$

$A_d = e^{AT}$, $B_d = \left(\int_0^T e^{A\tau}\, d\tau\right) B$

The load current dynamics of the four-leg inverter in (5) can be expressed as

$$i(t) = \frac{di}{dt} = Ai(t) + Bu(t)$$

$A = -\frac{R_{eq}}{L_{eq}}$, $B = \frac{1}{L_{eq}}$, $u(t) = v(t)$

Therefore, the load current dynamics of the electrical converter, expressed within the discrete-time domain with the discrete-time state-space equations are

$$i(k+1) = A_d i(k) + B_d v(k)$$

where $A_d = e^{AT_s}$, (32)

$$B_d = \left(\int_0^T e^{A\tau}\, d\tau\right) B = A^{-1}(A_d - I)B = -\frac{1}{R_{eq}}\left(e^{\frac{-RT_s}{L_{eq}}} - 1\right)$$

Based on the exact discrete-time domain, the load current dynamics with the discrete-time state-equation can be more precisely written in the discrete-time domain as

$$i(k+1) = e^{\frac{-R_{eq}T_s}{L_{eq}}} i(k) - \frac{1}{R_{eq}}\left(e^{\frac{-R_{eq}T_s}{L_{eq}}} - 1\right) v(k) \quad (33)$$

With assumption that one step future load currents become equal to the one-step future current references through the voltage reference application, the reference voltage vector may be expressed as

$$V(k)^* = \left\{ \frac{e^{\frac{-R_{eq}T_s}{L_{eq}}}}{(e^{\frac{-R_{eq}T_s}{L_{eq}}} - 1)/R_{eq}} \right\} i(k) \quad (34)$$

Owing to the fast sampling and the switching frequency of the inverter in this paper, the discrete-time modelling based on

the finite-difference method in (33), can be Simply implemented in this paper.

TABLE 4

Variable	Description	Value*
V_s	Source voltage	55[V]
f	System frequency	50[Hz]
v_{dc}	dc-voltage	162[V]
C_{dc}	dc capacitor	2200[μF](2.0 pu)
L_f	Filter inductor	5.0[mH](0.5 pu)
R_f	Internal resistance within L_f	0.6[Ω]
T_s	Sampling time	20[μs]
T_e	Execution time	16[μs]

Note: V_{base}=55v and S_{bace} = 1KVA

4SIMULATION RESULTS

A simulation model for the three-phase four-leg PWM converter with the parameters shown in Tablel-4 has been developed using MATLAB/SIMULINK environment and tested various loads for evaluating the various capabilities of the controller like load balancing, harmonic mitigation and improving the power factor of the overall power system. In the loads, three phase diode bridge rectifier feeding R load with series switch and across three phase diode bridge rectifier feeding R load is connected across the supply, single resistance switch is connected across the phase 'a' to neutral. The objective is to verify the current harmonic compensation effectiveness of the proposed control scheme under different operating conditions. A six-pulse rectifier was used as a nonlinear load and 1-phase R-load also be the unbalance and nonlinear load in shown Fig.11. The conventional

4.1 Conventional Predictive controller with 3-phase 4-Leg VSI

Fig.11. shows simulation model of APF with 4L-vsi using conventional predictive control system andsimulation resultsshown in Fig.12, the active filter starts to compensate the active power filter injects an output current i_{ou} to compensate current harmonic components, current unbalanced, and neutral current simultaneously. During compensation, the system currents are shown sinusoidal waveform Fig.13. at t =t_1(0.2 sec) , a three-phase balanced load 45Ω. The compensated system currents remain sinusoidal despite the change in the load current magnitude. Finally, at t=t_2(0.3 sec), a single-phase load 75Ω introduced in phase u. As expected on the load side, a neutral current flows through the neutral conductor (i_{Ln}), but on the source side, no neutral current is observed (i_{Sn}). Simulated results show that the proposed control scheme effectively eliminates unbalanced currents. Additionally, Fig. 5 shows that the dc voltage remains stable throughout the whole active power filter operation.

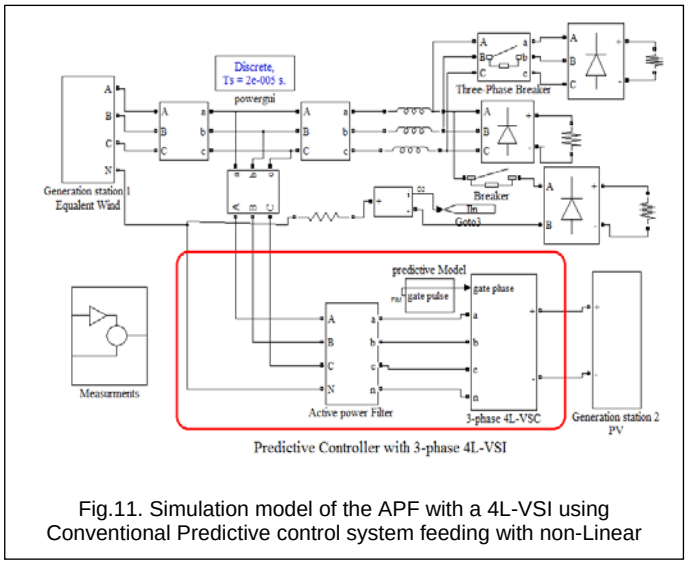

Fig.11. Simulation model of the APF with a 4L-VSI using Conventional Predictive control system feeding with non-Linear

Fig.12. shows the steady state performance of the proposed model feeding a three phase load of 45Ω and single-phase nonlinear load 75Ω across the phase 'a'. Due to the presence of the resistive load unbalance in both 3-phase non-linear at t=0.2sec and 1-phase non-linear load at t=0.3sec is created in the source voltage effect and due to the presence of non-linear load harmonics are injected into the source currents causing non- sinusoidal source current.

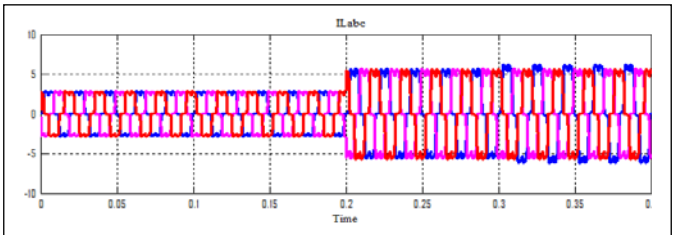

Fig.12(a). Three phase Load current (ILabc)

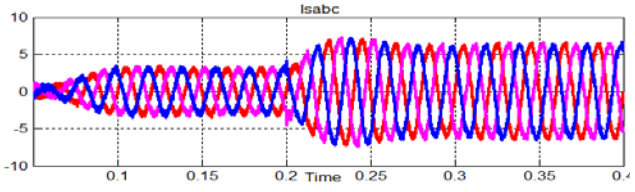

Fig.12(b). Three phase Source current (Isabc)

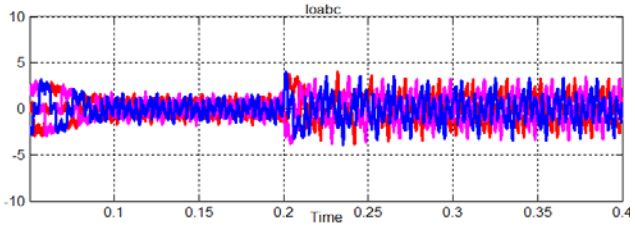

Fig:12(c). Three phase 4-leg VSI output current (Ioabc)

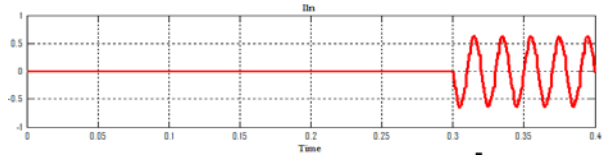

Fig.12(d). Single phase load current (Iln)

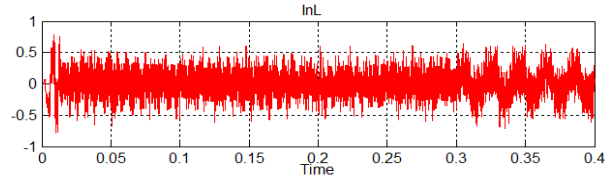

Fig.12(e). Three phase source neutral current at unbalanced Load(InL)

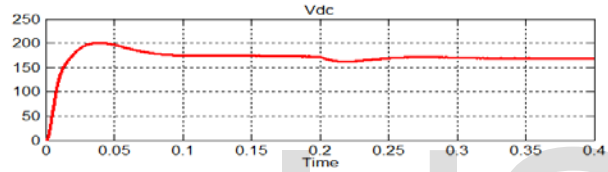

Fig.12(f). DC voltage of capacitance (Vdc)

Fig.12. Simulation waveforms of the using Conventional Predictive control system

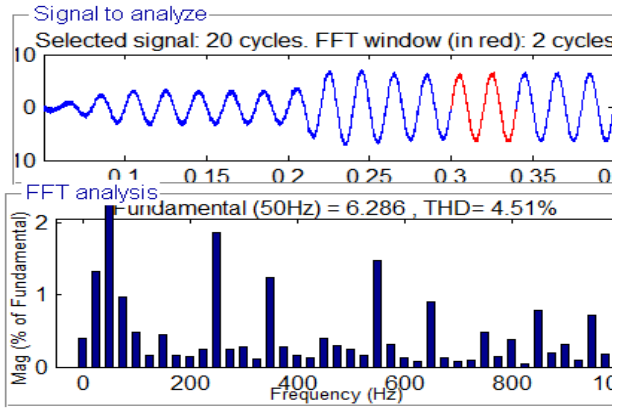

Fig.13.THD Analysis of source current Conventional Predictive control system

4.2 Proposed Predictive controller with 3-D SVPWM in 3-phase 4-Leg VSI

Fig.14. shows simulation model of APF with 4L-vsi using proposed predictive control system and Fig15. Shows Simulation model of the Predictive control system with 3-D SVPWM, simulation results shown in Fig.16, General expressions of the proposed transformation matrix $T_{\propto\beta 0z}$ and all the other classical transformation matrices $T_{\propto\beta 0}$ used in the literature and the V_n switching states vector obtained for each transformation matrix are given. Transformation matrix and switching states vector general expressions are shown in Table 5in the T and $\overline{V_n}$, respectively.

On time upper switches T_u , T_v, T_w , T_n were calculated in MATLAB for balanced linear/unbalanced nonlinear three-phase voltage signals by using each transformation matrix and the same 3-D SVPWM algorithm. Phase-neutral voltages were obtained again by synthesizing T_u, T_v, T_w , T_n with DC-line voltage V_{dc} and the results were comparedeven though the switch states vector V_n expressions are different for each transformation matrix, T_u, T_v, T_w, T_n and V_{un}, V_{vn}, V_{wn} calculated by the proposed transformation matrix and the other classical transformation matrices are the same. Simulation results prove the validity of the proposed 4*4 $T_{\propto\beta 0z}$ transformation matrix for 3-D SVPWM strategies with respect to the other algorithms.

Table 5

$T_{\alpha\beta 0z}$	$\overline{V_n} = V_{\alpha\beta 0z}$
$\frac{2}{3}\begin{bmatrix} 1 & -1/2 & -1/2 \\ 0 & \sqrt{3}/2 & -\sqrt{3}/2 \\ 1/\sqrt{2} & 1/\sqrt{2} & 1/\sqrt{2} \end{bmatrix}$	$\begin{bmatrix} \frac{2}{3} * d_\alpha \\ \frac{1}{\sqrt{3}} * d_\beta \\ \frac{\sqrt{2}}{3} * d_0 \end{bmatrix}$ *Vdc
$\sqrt{\frac{2}{3}}\begin{bmatrix} 1 & -(1/2) & -(1/2) & 0 \\ 0 & \sqrt{3}/2 & -(\sqrt{3}/2) & 0 \\ (1/(2*\sqrt{2})) & (1/(2*\sqrt{2})) & (1/(2*\sqrt{2})) & -(3/(2*\sqrt{3})) \\ (\sqrt{3}/(2*\sqrt{2})) & (\sqrt{3}/(2*\sqrt{2})) & (\sqrt{3}/(2*\sqrt{2})) & (\sqrt{3}/(2*\sqrt{2})) \end{bmatrix}$	$\sqrt{\frac{3}{2}}\begin{bmatrix} \frac{1}{3} * d_\alpha \\ \frac{1}{\sqrt{3}} * d_\beta \\ \frac{1}{3\sqrt{2}} * d_0 \end{bmatrix}$ *Vdc

Furthermore, it can also be applied to a three-phase four-leg VSI. The second study is the real-time application of 3-D SVPWM with the optimal digital control rule in three-phase four-leg in the VSI using the proposed 4*4 $T_{\propto\beta 0z}$ orthonormal transformation matrix.

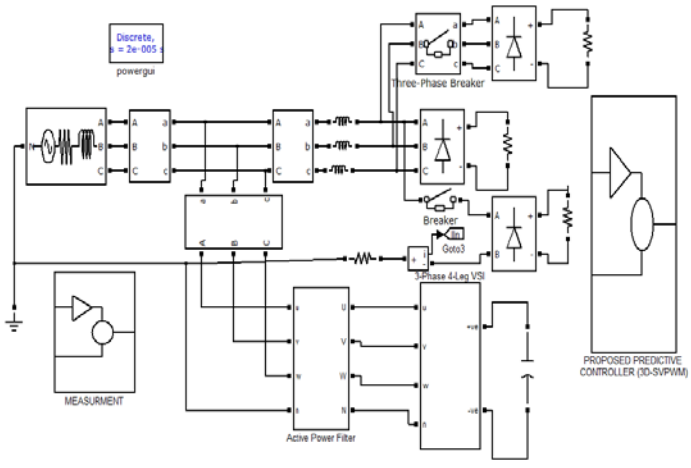

Fig.14. Simulation model of the APF with a 4L-VSI using Predictive control system with 3-D SVPWM feeding with non-Linear Load

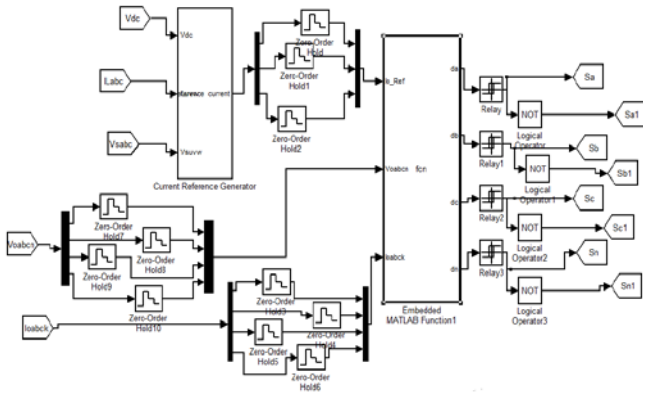

Fig.15.Simulation model of the Predictive control system with 3-D SVPWM

Nonlinear unbalanced load in this mode contains three different loads. The first one, balanced nonlinearload, consists of a three-phase diode bridge rectifier dc loadand the second one balanced nonlinear bridge rectifier dc load on at t_1=0.2sec the third was formed from a 1-phase linear load connected between phase-u and neutral at t_2=0.3sec. The load between the phases-u and neutral represents one ofthe unbalance conditions under which performances of the optimal digital control and 3-D SVPWM algorithms wereobserved. This study considers modelling the three-phase four-leg VSI in the abc coordinate system, discrete-time optimal controller design, full state space feedback control of VSI, and implementation of 3-D SVPWM via 4*4$T_{\alpha\beta 0z}$ transformation matrix

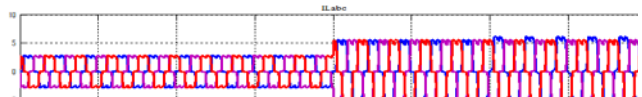

Fig.16(a):Three phase Load current (ILabc)

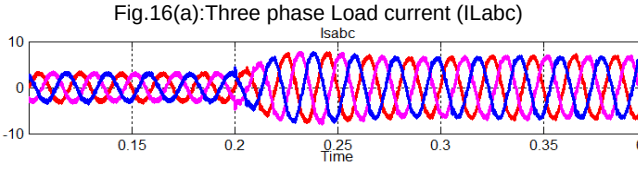

Fig.16 (b): Three phase Source current (Isabc)

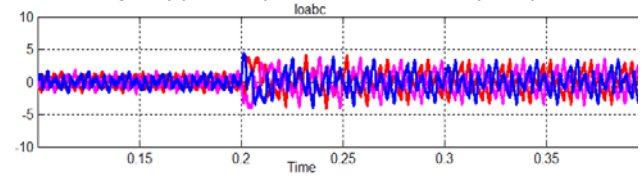

Fig:16 (c) Three phase 4-leg VSI output current (Ioabc)

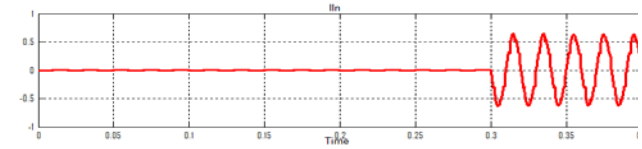

Fig.16 (d) Single phase load current (Iln)

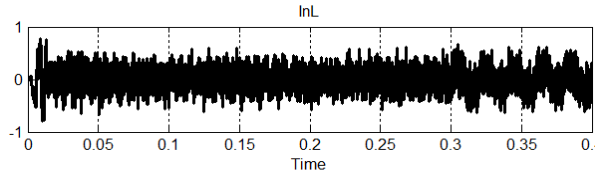

Fig.16 (e).Three phase source neutral current at unbalanced Load (InL)

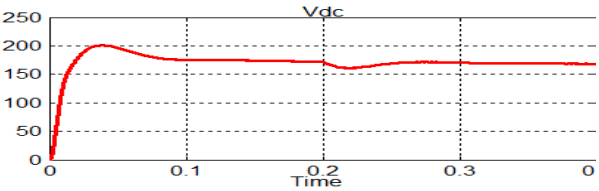

Fig.16 (f). DC voltage of capacitance

Fig.16. Simulation waveforms of the using Predictive control system with 3-D SVPWM

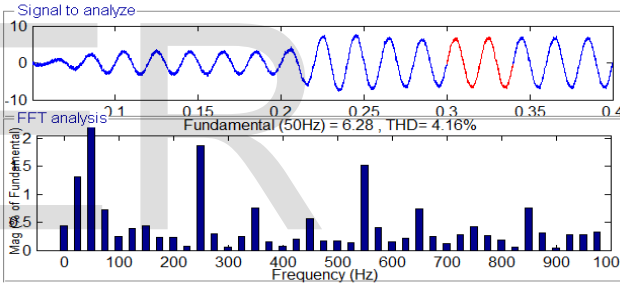

Fig.17.THD analysis of source current at Predictive control system with 3-D SVPWM

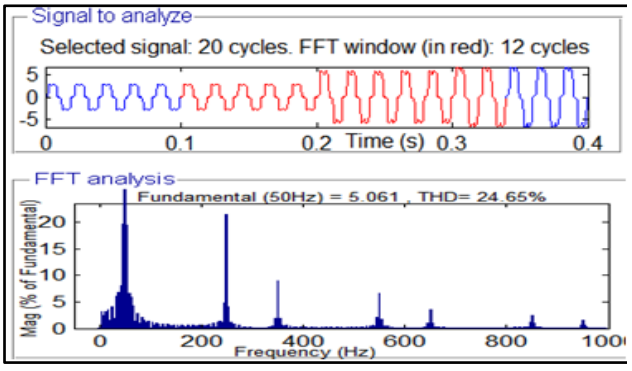

Fig.18. THD analysis of source current Without APF

The total harmonic distortion(THD) of the generating currents of given in Fig.18. It is found that THD of generating currents is far more than the required level as specified by the IEEE-519 standards, which should be less than 5%.

The total harmonic distortion (THD) of generating current is given in Fig.13 & 17. The THD of the source current is maintained below 5% as per the standards of the IEEE-519 with the help of APF with predictive controller and APF with Predictive controller with 3-D SVPWM action

TABLE 6
Percent of THD of the source current APF with predictive controller and APF with predictive controller with 3-D SVPWM technic at unbalanced load condition.

S.no	FEEDING WITH 1-PHASE AND 3-PHSE NON-LINEAR LOADS	THD OF SOURCE CURRENT
1	Without APF in unbalance load	24.68%
2	APF With Predictive controller in unbalanced load	4.51%
3	APF with Predictive controller with 3-D SVPWM technique in unbalanced load	4.16%

5 Conclusion

This paper proposes a simplified model predictive control method based on a future reference voltage vector for a three phase four-leg VSI. The proposed technique can preselect three active voltage vectors among the entire 14 possible active voltage vectors produced by the three-phase four-leg VSI based on the position of the future reference voltage vector. The discrete-time model of the future reference voltage vector is established to predict the future movement of the load currents, and its position is used to choose three preselected active vectors at every sampling period. As a result, the proposed method can reduce calculation load by decreasing the candidate voltage vectors used in the cost function for the four-leg VSIs, while exhibiting the same performance as the conventional method. The effectiveness of the proposed method is demonstrated with simulation results.

References

[1] M. Ryan, R. Lorenz, and R. De Doncker, "Modeling of multi-leg sine-wave inverters: A geometric approach,"IEEE Trans. Ind. Electron., vol. 46, no. 6, pp. 1183–1191,Dec. 1999..

[2] J. Huang, R. Xiong, Z. Wang, W. Zuo, Y. Zhou, and H.Shi, "A novel SPWM control strategy to reduce commonmode voltage in three-phase four-leg inverters," in Proc.IEEE ICEMS Conf., Wuhan, China, Oct. 2008, pp. 1526–1530.

[3] [3] J.-H. Kim and S.-K.Sul, "A carrier-based PWM methodfor three-phase four-leg voltage source converters," IEEETrans. Power Electron., vol. 19, no. 1, pp. 66–75, Jan.2004.

[4] J.-H. Kim, S.-K. Sul, and P. N. Enjeti, "A carrier-basedPWM method with optimal switching sequence for amultilevel four-leg voltage-source inverter," IEEE Trans.Ind. Appl., vol. 44, no. 4, pp. 1239–1248, Jul. 2008.

[5] Y. Kumsuwan, W. Srirattanawichaikul, S.Premrudeepreechacharn, K. Higuchi, and H. Toliyat, "Acarrier-based unbalanced PWM method for four-legvoltage source inverter fed asymmetrical two-phaseinduction motor," in Proc. IEEE IPEC Conf., Singapore,Jun. 2010, pp. 2469–2476.

[6] N.-Y. Dai, M.-C.Wong, F. Ng, andY.-D.Han, "A FPGAbasedgeneralized pulse width modulator for three-legcenter-split and four-leg voltage source inverters," IEEETrans. Power Electron., vol. 23, no. 3, pp. 1472–1484,May 2008.

[7] S. L. Salazar, H. F. Zapata, and F. E.Weichmann,"Analysis, design and experimental evaluation of a fourpolePWM rectifier using space vector modulation," inProc. IEEE-PESC'97 Conf., 1997, pp. 484–490.

[8] R. Zhang, V. Prasad, D. Boroyevich, and F. Lee, "Threedimensional space vector modulation for four-leg voltagesource converters," IEEE Trans. Power Electron., vol. 17, no. 3, pp. 314–326, May 2002.

[9] M. Zhang, D. J. Atkinson, B. Ji, M. Armstrong, and M. Ma,"A near state three dimensional space vector modulationfor a three phase four leg voltage source inverter," IEEETrans. Power Electron., vol. 29, no. 11, pp. 5715–5726,Nov. 2014.

[10] J. Rodriguez, J. Pontt, C. A. Silva, P. Correa, P. Lezana, P.Cortes, and U. Ammann, "Predictive current control of avoltage source inverter," IEEE Trans. Ind. Electron., vol.54, no. 1, pp. 495–503, Feb. 2007.

[11] S. Moon and S. Kwak, "Reducing Common-Mode Voltageof Three-Phase VSIs with Predictive Current ControlMethod without Cost Function,"Journal of PowerElectronics, vol. 15, no. 3, pp. 712-720, May. 2015.

[12] S. Kwak and J. Park, "Predictive Control Method withFuture Zero-Sequence Voltage to Reduce SwitchingLosses in Three-Phase Voltage Source Inverters," IEEETransactions on Power Electronics, vol. 30, no. 3, pp. 1558-1566, Mar. 2015.

[13] V. Yaramasu, M. Rivera, B. Wu, and J. Rodriguez,"Model predictive current control of two-level four-leginverters-part I : concept, algorithm and simulationanalysis," IEEE Trans. Power Electron., vol. 28, no. 7, pp. 3459–3468, Jul 2013.

[14] [15] P. Cortes, J. Rodriguez, C. Silva, and A. Flores, "Delaycompensation in model predictive current control of athree-phase inverter," IEEE Trans. Ind. Electron., vol. 59,no. 2, pp. 1323–1325, Feb. 2012.

[15] A. Ziani, A. Llor, and M. Fadel, "Model predictive current controller for four-leg converters under unbalancedconditions," in Proc. IEEE Eur. Conf. Power Electron.and Appl., Birmingham, U.K, Sep. 2011, pp. 1–10.

[16] M. Rivera, V. Yaramasu, A. Llor, J. Rodriguez, B. Wu,and M. Fadel, "Digital predictive current control of athree-phase four-leg inverter," IEEE Trans. Ind. Electron.,vol. 60, no. 11, pp. 4903–4912, Nov. 2013.

[17] R. L. A. Riberio, C. B. Jacobina, E. R. C. da Silva, and A.M. N. Lima, "Fault-tolerant voltage-fed PWM inverter ACmotor drive systems," IEEE Trans. Ind. Electron., vol. 51,no. 2, pp. 439–446, April 2004.